

# Applications of wavefront division interferometers in soft x rays

F. Polack

LURE, CNRS, CEA, MESR, Centre Universitaire, Bat. 209D, 91405 Orsay Cedex, France

D. Joyeux, J. Svatoš, and D. Phalippou

Institut d'Optique, B. P. 147, 91403 Orsay Cedex, France

(Presented on 21 July 1994)

The development of soft x-ray interferometry demands high quality optical elements and high brightness sources. However, the balance between these two requirements depends on the exact nature of the interferometer setups. Generally speaking, amplitude division interferometers require beam splitters, the optical quality of which remain a big technological issue. On the contrary, the high brightness sources needed by wavefront division interferometers are readily available, and will progress in the near future. Examples of such interferometers are given for various applications in development or in project. © 1995 American Institute of Physics.

## I. INTRODUCTION

Interferometry in the x-ray domain has basically the same virtualities than in any other spectral range, and the fact it is not developed for short wavelengths is due to the particular difficulties of instrumental soft x-ray (SXR) optics: lack of high quality optical elements, small number of available high brightness x-ray sources. Historically, hard-x-ray interferometers have been constructed long before soft x-ray ones, because large silicon single crystals are easily available and make high quality reflectors and beam splitters in the 1 Å wavelength range.<sup>1</sup> However, in the past years a number of coherent soft x-ray experiments have been done, among which a few were truly interferometry (Gabor and Fourier transform holography.<sup>2-4</sup>) Then emerged the idea that soft x-ray interferometry could be extended to a full range of applications, as it is in visible optics, provided convenient interferometers are designed. First, following an early experiment by Aoki,<sup>5</sup> the Fresnel bi-mirror was used by our group to measure actual soft x-ray refractive indices<sup>6,7</sup> and later we proposed to use it in a SXR scanning microscope to image phase objects.<sup>8</sup> Quite recently, it has been suggested<sup>9,10</sup> that Fourier transform (FT) spectroscopy could be implemented in the SXR range and yield very high resolutions (>100 000) which are completely out of reach of other kind of spectrographs.

All these applications need interferometers adapted to the available SXR optical elements and sources. We show in examples how wavefront division interferometers can meet the requirements with only presently available technology.

## II. WAVEFRONT DIVISION VERSUS AMPLITUDE DIVISION INTERFEROMETERS

One key point of designing an interferometer is to use only the highest grade optical elements which can be manufactured, because the interfering wavefronts should be perfected to a much smaller fraction of the working wavelength than in diffraction limited imagery. In soft x rays, the tolerances can be very tight though the use of grazing incidence somewhat relaxes them (by  $1/\text{grazing angle}$ ), but the special conditions of SXR optics considerably restrict the design possibilities. One major issue of SXR optical technology is

to fabricate beam splitters of interferometric quality, and, despite clever devices have been proposed,<sup>9,10</sup> the feasibility of such devices is not proved up to now. Therefore, it is important to ask whether it is wise to develop an interferometer with beam splitters or, try to do without it, that is to say preferring a wavefront division to an amplitude division interferometer.

The great advantage of a beam splitter is to perform a so-called amplitude division of a wavefront. If available with the required quality, they would allow to have almost no separation between interfering rays. Therefore, it would be possible to use an extended incoherent source. If beam splitters are not available, we then must use a wavefront division interferometer, where the interfering waves are generated by taking separate parts of a primary wavefront, as in the Young slit setup. These setups require a spatially coherent illumination, the minimum partial coherence area being the size of the ray separation.

A particular degree of spatial coherence can always be realized even from a completely incoherent source, by selecting with a pinhole, a small part of the source in such a way that the angular beam separation is smaller than the diffraction cone from the pinhole (Zernike-Van Cittert theorem). Very high brightness sources, as undulators, are required to have enough flux in the reduced étendue but, it is worth saying that the last generation of the high brightness storage ring, almost achieve to be naturally coherent in one direction at least, for wavelengths of 10 nm or more. For instance, an insertion device with a source size of 10  $\mu\text{m}$  (FWHM) will have, for 10 nm radiation, a coherent aperture of roughly 0.2 mrad, i.e., 4 mm width at 10 m.

Therefore, present synchrotron sources do allow the implementation of wavefront division interferometers without beam splitters. For the other optical elements, it is advisable to use plane mirrors only, because flat surfaces are those which can be manufactured with the highest accuracy. Less than  $\lambda/300$  (visible wavelength) can be achieved (rather easily a few  $\text{cm}^2$  surfaces). Thanks to the grazing incidence, it corresponds to a  $\lambda/30$  accuracy for a 10 nm wavefront and a  $6^\circ$  grazing angle.

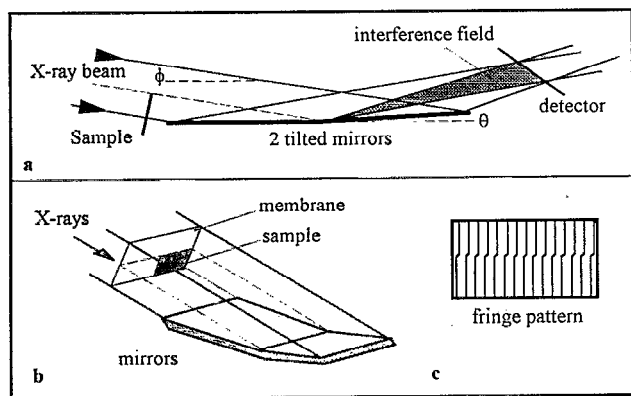


FIG. 1. Fresnel bi-mirror setup for index measurements. (a) General principle for producing fringes, (b) mirrors and sample arrangement, and (c) resulting fringe pattern.

### III. SOME APPLICATIONS OF SOFT X-RAY INTERFEROMETRY

#### A. Direct measurement of refractive index

The real part  $\delta$  of the SXR index of refraction ( $n=1-\delta-i\beta$ ), is known either by computing an integral transform over the absorption factors, or from reflectivity measurements. It is not always reliable, especially near the edges but accurate figures are needed for calculating the thin-film optical element as multilayers, Fresnel lenses of any kind, or phase shifters. The measurement of the near-edge behavior of refractive index, especially the width and depth of the anomalous region where  $\delta$  can be negative, is a good test of atomic models.<sup>11</sup> We also believe that near-edge index fine structures could also yield valuable information.

Direct measurement of the refractive index can be done by inserting a thin sample into one way of an interferometer. If it is set up to display a parallel fringe pattern, the change in optical path difference (OPD) will shift the pattern, and from this shift it is easy to obtain the optical thickness with good accuracy. The schematic of the Fresnel bi-mirror interferometer we use at Super-ACO is given in Fig. 1. Interferences are produced in the region where the two reflected beams overlap. The angle between mirrors is  $\theta=2.25$  arcmin, giving a fringe spacing of  $3 \mu\text{m}$  at  $4 \text{ nm}$  wavelength. Inclining the detector enlarges the apparent spacing by a factor close to 10 so that it can be recorded on a photoplate. The spatial coherence is given by the  $0.125 \text{ mm}$  exit slit of the monochromator  $10 \text{ m}$  in front of the interferometer, and rays separated by  $0.16 \text{ mm}$  have a mutual coherence over  $0.8$ ; more than 50 fringes can be recorded with this contrast.

Processing and digitization of the photoplate allow to determine the shift with an accuracy of  $0.015$  period. The corresponding accuracy on the index value is  $2 \times 10^{-5}$ . The result of the analysis of 10 interferograms is given in Fig. 2. It shows the index of a carbon containing resist near carbon edge. The region of negative  $\delta$  values is clearly visible. We are now working to replace the photoplate by a moiré real time detection. UV simulations with the device let us expect an accuracy much better than  $1/100$  fringe in the shift determination.<sup>12</sup>

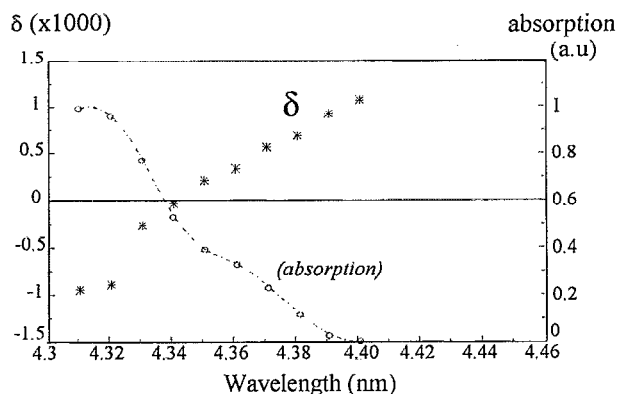


FIG. 2. Plot of measured values of the refractive index of a resist near carbon  $K$  edge. The measure absorption is given as a wavelength reference.

#### B. Interferential differential scanning microscopy

Scanning transmission x-ray microscopes (STXM) normally provide pure absorption images. There is however a growing interest for phase microscopy, mainly for its expected ability to reduce the damages from energy absorption. We have recently proposed to include an interferometric setup within an existing STXM, in order to produce a differential phase contrast. This setup is sketched in Fig. 3. It consists of illuminating the sample with two close spots, mutually coherent, instead of one. They produce a pattern of several fringes in the objective and detector planes. If the detector is shaped in order to detect the flank of one fringe, it is sensitive to small fringes shifts and the setup is able to detect phase steps between the spots or phase slopes. The double spot can be produced by simple wavefront division interferometers such as Fresnel mirrors or Young slits.

A first test of the setup has been carried out a few months ago on the STXM of SUNY-Stony Brook, on the X1A line of the Brookhaven NSLS facility, in collaboration with Chris Jacobsen. Young slits, with an aspect ratio  $1/1$ , were used to produce two spots separated by one diffraction radius ( $0.05 \mu\text{m}$ ). The observed fringe profile was close to the theoretical  $\text{sinc}^2(x)$  modulated cosine profile and the  $0.8$  contrast of the central fringe is in good agreement with the value estimated from beam-line data. Images of polyimide slabs,  $1.1 \mu\text{m}$  thick,  $\sim 0.5 \mu\text{m}$  wide,  $\sim 0.9 \mu\text{m}$  spacing,<sup>13</sup> have been done with and without the phase sensitive detection. Figure 4 shows an average of such image profiles over 90 lines. Due to the strong absorption of the object, the phase effect consist of the small overshoot visible in Fig. 4(b).

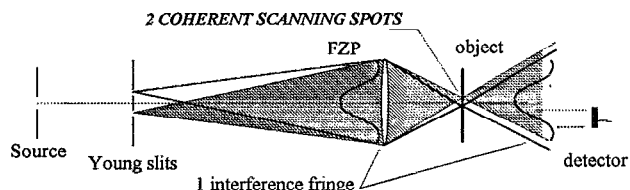


FIG. 3. Soft x-ray scanning interferential differential microscopy setup. Two coherent spots probe the phase slopes or steps of the specimen.

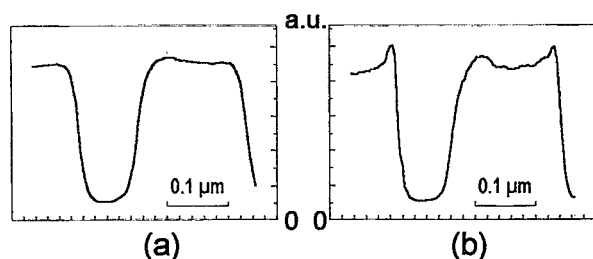


FIG. 4. Signal profiles of STXM images of polyimide slabs ( $1.1 \mu\text{m}$  thick): (a) energy transmission (without phase sensitive detection), (b) energy and phase signal with phase sensitive detection. Profiles are averaged on 90 image lines.

### C. Soft x-ray Fourier transform spectroscopy

The possibility of extending FT spectroscopy to the XUV and SXR range has received much consideration in the very recent years. Let us recall that when the OPD between the two ways of an interferometer is varied, the fringe modulation envelope is the FT of the spectrum of the source (in wave number unit). For XUV and SXR applications the important property is that the smallest resolved spectral element is related to the maximum OPD allowed by the interferometer. OPD of a few mm do not look that difficult to achieve and would yield a resolution in the order of 100 000 in the 10–50 nm wavelength range. This value, which is not a limit, is already far beyond the present possibilities of grating monochromators.

The implementation considered in Ref. 10 is based on a Mach–Zehnder geometry. The setup only uses flat mirrors but includes beam splitters which, as we said before, we consider as the weak part. Instead, with K. D. Möller, we suggest a wavefront division interferometer the principle of which is given in Fig. 5. It uses two pairs of mirrors, roof shaped with a large roof angle. One is fixed and the other can be translated along the angle bisector in such a way that only the optical path is changed but not the position of the reflected ray [Fig. 5(b)]. The mirrors are slightly tilted sideways, allowing the beams from the two ways to overlap and interfere. In this configuration, the separation between interfering rays, i.e., the required spatial coherence is constant in the field and also remains constant when the mirrors are moved. It is not useful to recombine the beams in order to get a uniform interference; only the detector needs to be smaller than  $\sim 1/4$  the fringe spacing. The beam energy is best used when the beam size compares with the fringe spacing, and it implies that the beam is almost coherent in one direction.

Many synchrotron sources are able to deliver a 1D-coherent photon flux greater than the  $10^{10}$  photons per second per 0.1% bandwidth which is enough to record good spectra with a resolution of  $10^5$ .<sup>10</sup> With a 10 cm long roof used at  $\alpha=6^\circ$  grazing incidence, a 2 mm OPD (i.e., a resolution of  $4 \times 10^5$  at  $\lambda=10$  nm) can be reached. The configuration is fairly immune to translation errors because the variations of OPD with mirrors rotations are all second order. The grazing incidence also reduces the demand on position-

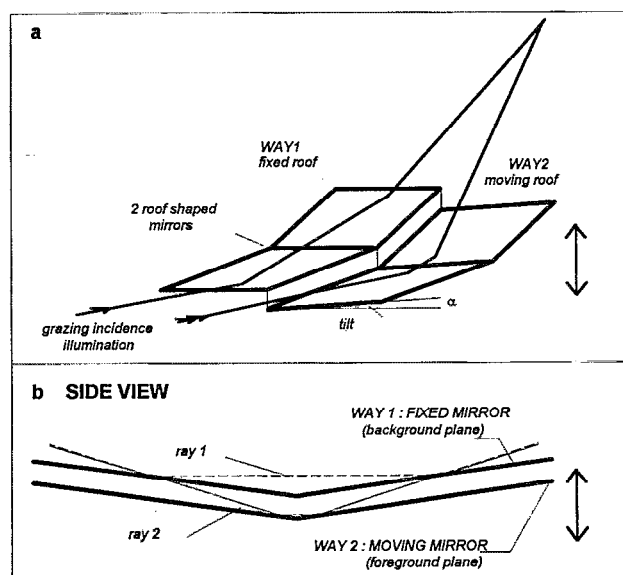


FIG. 5. A wavefront division interferometer proposed for XUV FT spectroscopy (a) 3D sketch showing the path in each way; (b) side view showing there is no position change of the emerging ray when mirrors are moved, if the roof angle is twice the incidence angle.

ing accuracy, e.g., an OPD error of 1 nm is achieved with 2.5 nm accuracy in the movement direction and 7 nm in the perpendicular one. It is definitely within the capacities of visible light interferometers.

### D. Ultrafine structures

Well contrasted, extremely fine interference fringes (say under 10 nm period) have never been produced in XUV, though they might be useful in various metrology applications, e.g., testing photoresists resolution,<sup>14</sup> measuring grating profiles, etc. Such fine fringes (with adjustable spacing optionally) can be obtained with a simple two mirror interferometer as shown in Fig. 6. The angle between interfering beams is four times the grazing angle, which allows rather small fringe periods to be achieved whenever the grazing angle remains small enough for keeping a high reflection factor on metal coatings. At  $\lambda=2$  nm for instance, a fringe spacing of 7 nm is obtained with a  $4^\circ$  grazing angle, at which a Ni coated mirror still has  $\sim 50\%$  reflectivity. Because the setup is symmetric, the interferences are produced near the zero OPD, and the beam intensities are balanced. This en-

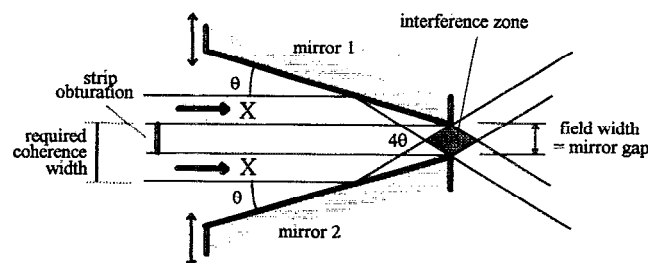


FIG. 6. A two mirrors setup suitable for producing contrasted ultrafine fringes for high resolution metrology.

sure a good contrast provided the spatial coherence condition, coherence area larger than twice the mirror gap, is fulfilled. The fringe spacing can be adjusted by changing the mirror angle symmetrically, which could be done with flexural hinge based mechanics.

#### IV. CONCLUSION

We have presented a few applications of interferometry in the XUV and SXR wavelength range, some in development and others still in project. Other developments of SXR interferometry are also expected in the field of optical testing (shearing interferometry and related Ronchi method).<sup>15</sup> In most cases, wavefront division interferometers offer a simple solution, which without compromising on performances, is immediately realizable with current technology. Progress toward very small emittance SXR sources will make them even more efficient in the near future.

#### ACKNOWLEDGMENTS

The authors are indebted to many persons for the projects and realizations presented here. They are grateful to M. F. Ravet and co-workers of L2M (CNRS, France) for preparing the samples for index measurements. Experiments on interferential phase contrast microscopy could not have been done without the collaboration and assistance of Janos Kirz, Chris Jacobsen, and their collaborators of SUNY and NSLS. The authors especially acknowledge the invaluable help of H. Chapman. They are most grateful to K. D. Möller

(Fairleigh Dickinson University, NJ) to have called their attention to FT spectroscopy, and for his help in elaborating the concept of the interferometer presented here.

<sup>1</sup>U. Bonse, H. Lotsch, and A. Henning, *J. X-Ray Sci. Technol.* **1**, 107 (1989).

<sup>2</sup>M. Howells, C. Jacobsen, J. Kirz, R. Feder, K. McQuaid, and S. Rothman, *Science* **238**, 514 (1987).

<sup>3</sup>D. Joyeux, S. Lowenthal, F. Polack, and A. Bernstein, in *X-Ray Microscopy II*, edited by D. Sayre, M. Howells, J. Kirz, and H. Rarback (Springer, Berlin, 1988), p. 246.

<sup>4</sup>I. McNulty, J. Kirz, C. Jacobsen, E. H. Anderson, M. R. Howells, and D. P. Kern, *Science* **256**, 1012 (1992).

<sup>5</sup>S. Aoki and S. Kikuta, *AIP Conf. Proc.* **47**, 49 (1986).

<sup>6</sup>J. Svatos, D. Joyeux, D. Phalippou, and F. Polack, *Opt. Lett.* **18**, 1367 (1993).

<sup>7</sup>J. Svatos, D. Joyeux, F. Polack, and D. Phalippou, in *X-Ray Microscopy IV*, edited by A. I. Erko and V. V. Aristov (Bogorodski Pechatnik, Chernogolovka, Moscow, 1994).

<sup>8</sup>F. Polack and D. Joyeux, in *X-Ray Microscopy IV*, edited by A. I. Erko and V. V. Aristov (Bogorodski Pechatnik, Chernogolovka, Moscow, 1994).

<sup>9</sup>M. R. Howells, Z. Hussain, D. A. Shirley, A. Thorne, D. Möller, E. J. Moler, and W. Yun, *Soft X-ray Interferometry*, Workshop Report LBL-3451 Conference-9306201, Lawrence Berkeley Laboratory, Berkeley, CA, 1993.

<sup>10</sup>M. R. Howells, K. Frank, Z. Hussain, E. J. Moler, T. Reich, D. Möller, and D. A. Shirley, *Nucl. Instrum. Methods A* **347**, 182 (1994).

<sup>11</sup>C. T. Chantler, *Radiat. Phys. Chem.* **41**, 759 (1993).

<sup>12</sup>D. B. Bradshaw, Project Report for the award of Master of Engineering, University of Southampton, 1994.

<sup>13</sup>Part of a polyimide Zone plate, courtesy G. Schmahl.

<sup>14</sup>M. Howells (private communication).

<sup>15</sup>Z. Tan, A. A. McDowell, B. Lafontaine, J. E. Bjorkholm, R. R. Freeman, M. Himel, D. Tennant, D. Taylor, O. R. Wood II, W. K. Waskiewicz, D. L. Windt, D. L. White, and S. Spector, these proceedings.